From AGB Stars to Aspherical Planetary Nebulae

Recent Observational Highlights from the Far-IR and (Sub)mm to X-Rays

Part 1

Raghvendra Sahai

JPL, California Institute of Technology

Main Collaborators: M. Morris (UCLA), C. S'anchez Contreras (IEM-CSIS, Spain), M. Claussen (AOC/NRAO), C-F. Lee (ASIAA, Taiwan), N. Patel (CfA), Rolf Guesten (MPIfR/Bonn)

Funding: (a) NASA Astrophysics Data awards (b) HST/ STScI GO awards (c) Chandra GO awards (d) SOFIA GO awards

Outline

- (Background) **The formation of Aspherical Structure in Planetary Nebulae**

(note: this material covered in SOFIA teletalk on 4/27/11)

- **Recent (selected) Observational Highlights**

from (sub)mm and far-IR to UV, X-Rays

2 community-wide large projects on PNe (X-Rays, Far-IR)

- **Using SOFIA/GREAT to study the 3D Structure of PNe:** "Ring Nebula" NGC6720

Ordinary Stars (~1-8 Msun)

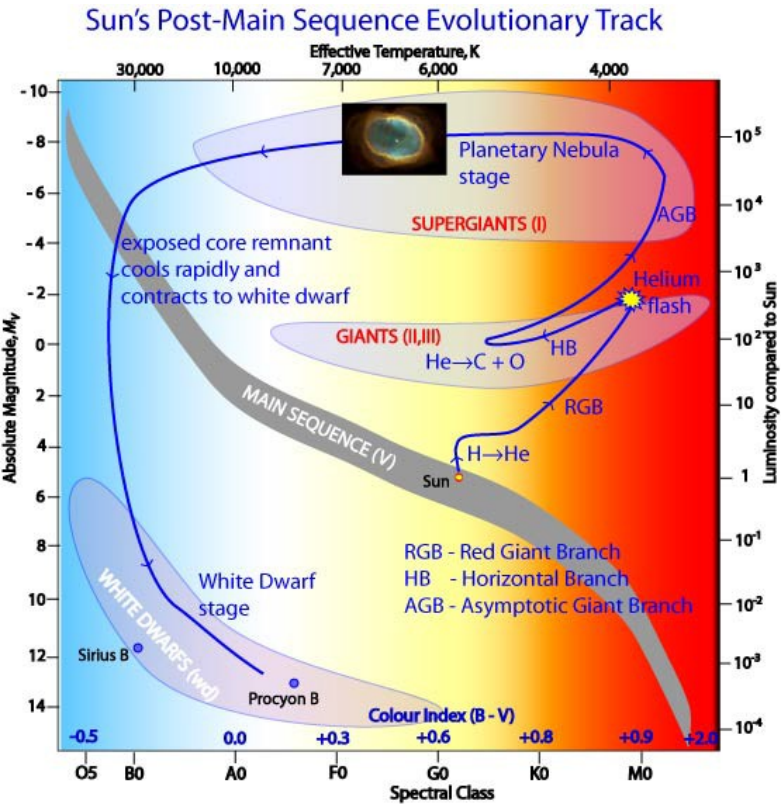

(outreach.atnf.csiro.au)

AGB phase

- Central (C+O) degenerate core, surrounded by He & H-shells (where nuclear-burning occurs), and a very large H stellar envelope
- cool (Teff < ~3000K), very luminous (~10^4 Lsun), have dusty, spherical expanding envelopes at low speeds (~5-20 km/s), but very large mass-loss rates (upto ~10^{-4} Msun/yr)
- *3 chemistry types: O-rich, S-type, C-rich (C/O <1, ~1, >1)*

(*winds can be driven by radiation pressure on dust grains; grains drag the gas along via friction: radiative momentum L/c > ~ dM/dt x Vexp,* but notable EXCEPTIONS, e.g., the Boomerang Nebula)

The Extraordinary Deaths of Ordinary Stars

- After most of the stellar envelope is lost due to mass-loss, heavy mass-loss ceases
- central star begins its post-AGB evolution (towards hotter Teff) at constant L
- A planetary nebula (PN) is formed when Teff~30,000K by the ionization of the molecular outflow

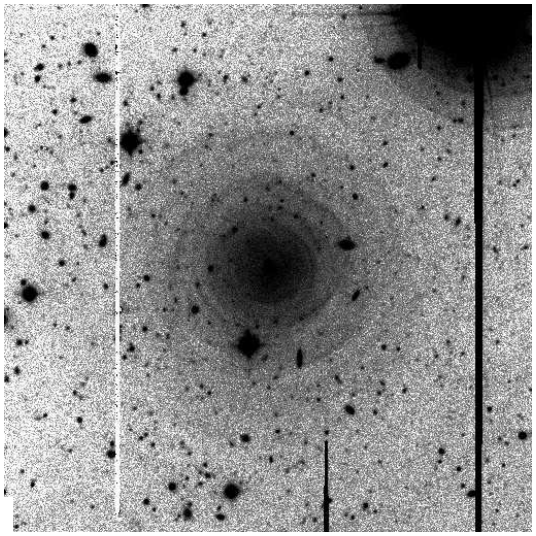

Circumstellar envelope of the **AGB star IRC+10216** illuminated by Galactic starlight (CFHT V-band: Mauron & Huggins 2000)

IRC10216 center

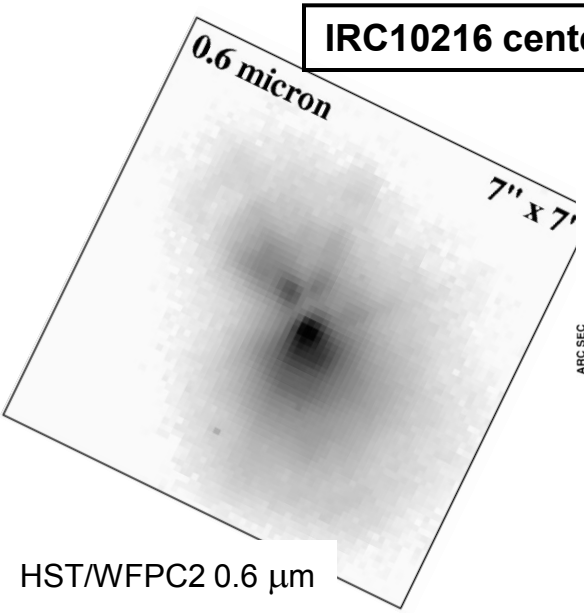

HST/WFPC2 0.6 μm

HCN J=3-2 (v=0,1,0), greyscale: continuum

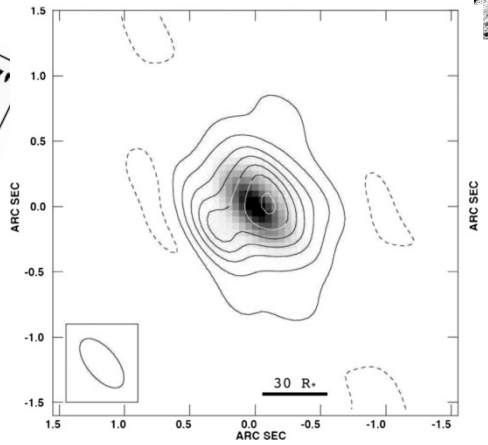

eSMA: 4 hr integration, baselines 25-782 m, beamsize 0.4"x0.22" (Shinnaga et al. 2009)

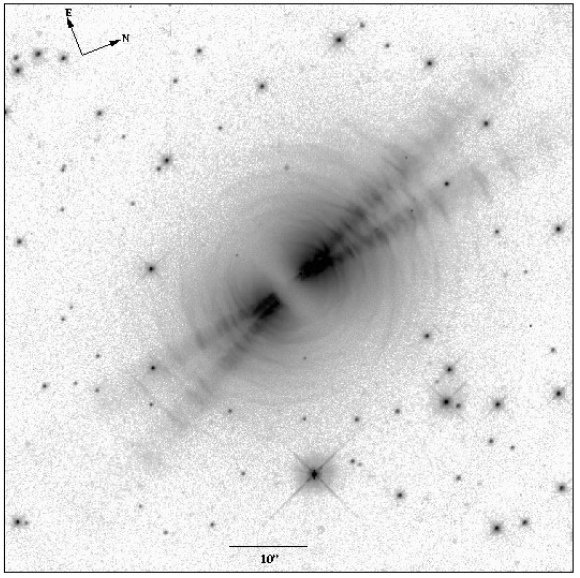

CRL2688 (C-rich PPN) *(Sahai et al. 1998a)*

The **PPN, CRL2688**, as seen in scattered light (HST, 0.6 μm) Sahai+1998

Dramatic transformation in the morphology and outflow velocity (~100 km/s) of the mass ejecta during the tranisition phase – the pre-planetary nebula (PPN) phase; process likely initiated during late-AGB phase

Imaging Surveys: nPPNe, PPNe, and PNe

Three morphologically-unbiased HST surveys (*using rather simple selection criteria*) have observationally bracketed the evolutionary phase over which the transition from spherical symmetry to asphericity occurs:

1. Young PN survey(s) (compact, [OIII]/Hα < ~1) (*e.g., Sahai & Trauger 1998; Sahai 2001-04 [IAU, APN meetings], Sahai, Morris & Villar 2011*)

2. Young PPN survey (*Sahai, Morris, Sanchez Contreras & Claussen 2007*)
[stars with heavy mass-loss: OH/IR stars (maser flux > 0.8 Jy) and C-rich objects; F25 > 25 Jy, IRAS F25/F12 > 1.4 i.e., lack of hot dust - AGB mass loss has stopped]

3. Nascent PPN survey [same as in (2), but 1 < F25/F12 < 1.4: earliest phase in PPN evolution] (*Sahai et al. 2010*)

Nascent PPNs (nPPNs)

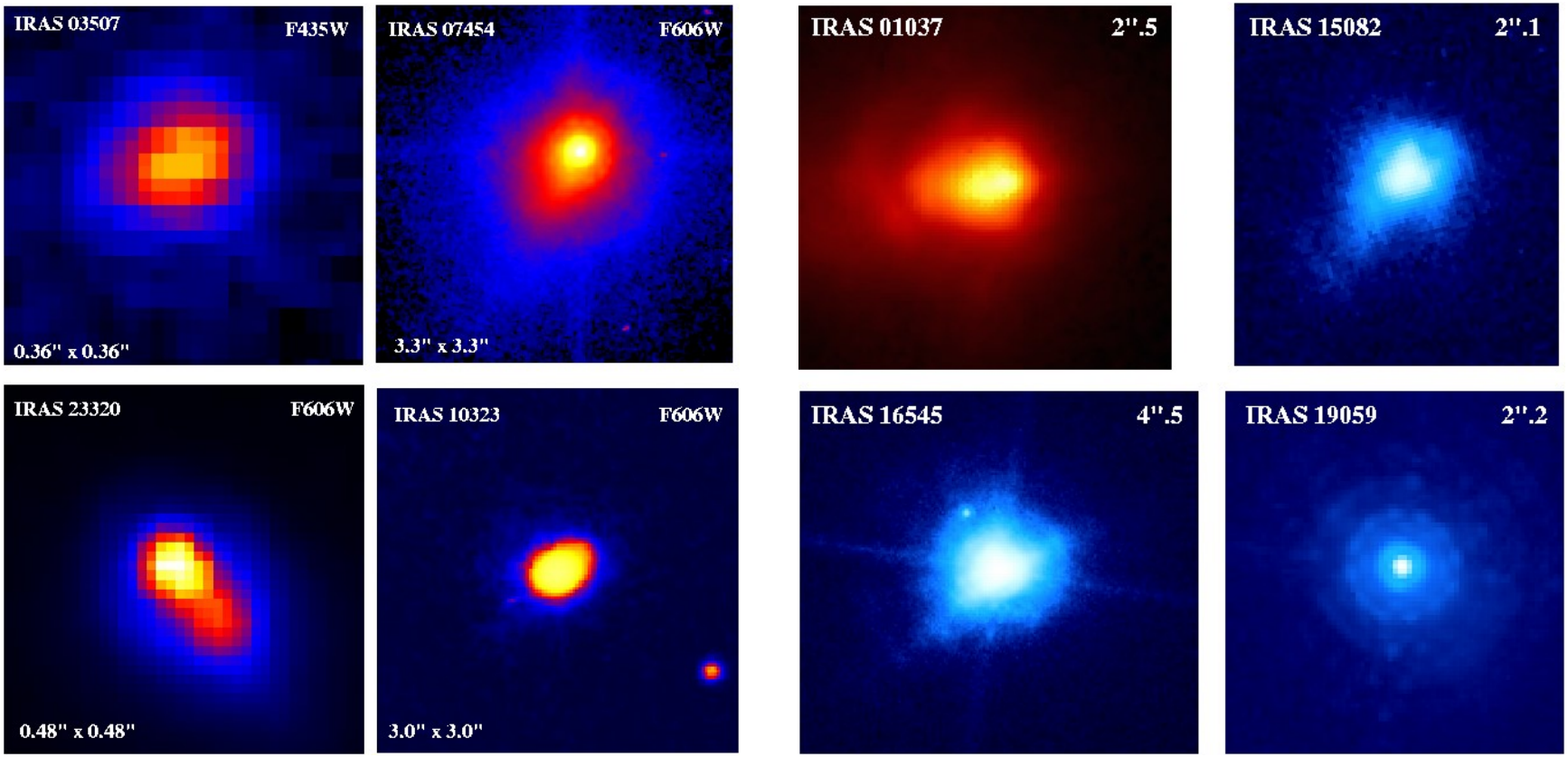

45 nPPNe were imaged. 30% of these are resolved - aspherical structure is seen in 60% of the resolved objects

In **our PPN survey**, fully 50% of our sample of 52 showed resolved morphologies, all of which were aspherical. The aspherical structure in the nPPN images (generally one-sided when collimated structures are seen) is very different from that observed in normal PPNs, which show diametrically-opposed, limb-brightened lobes.

HST Survey of Preplanetary Nebulae (PPNe)

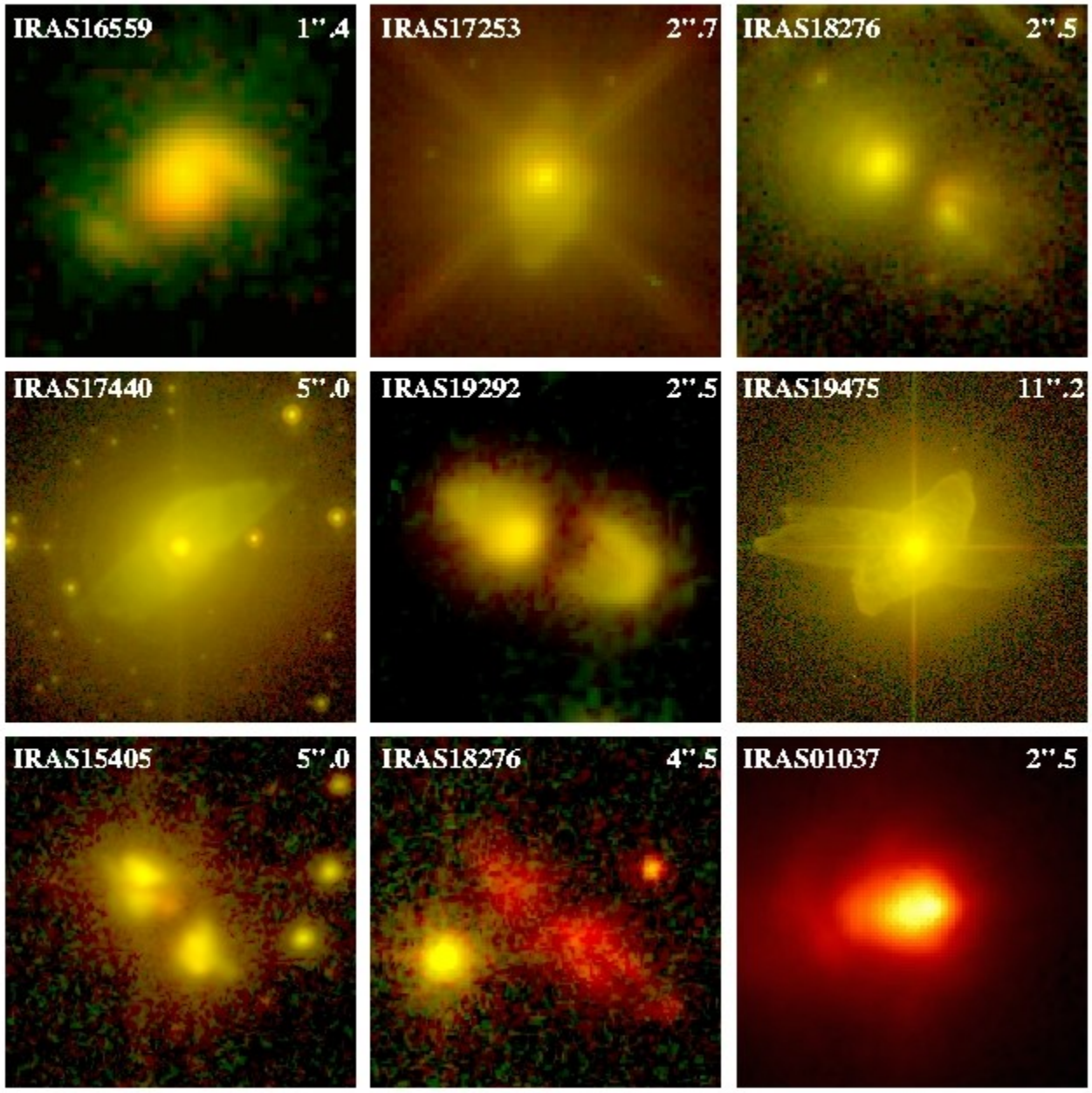

(Sahai, S'anchez Contreras, Morris, Claussen, AJ, 2007)

Morphological classification scheme for PPNe

Primary nebular shape

Bipolar, **M**ultipolar

Elongated, **I**rregular

Secondary descriptors: e.g., dusty waist, point-symmetry, halo

Important Point-Symmetric objects are NOT A PRIMARY CLASS

Point-symmetry found in all classes, except I(rregular)

PNs: Primary Class B (bipolar)

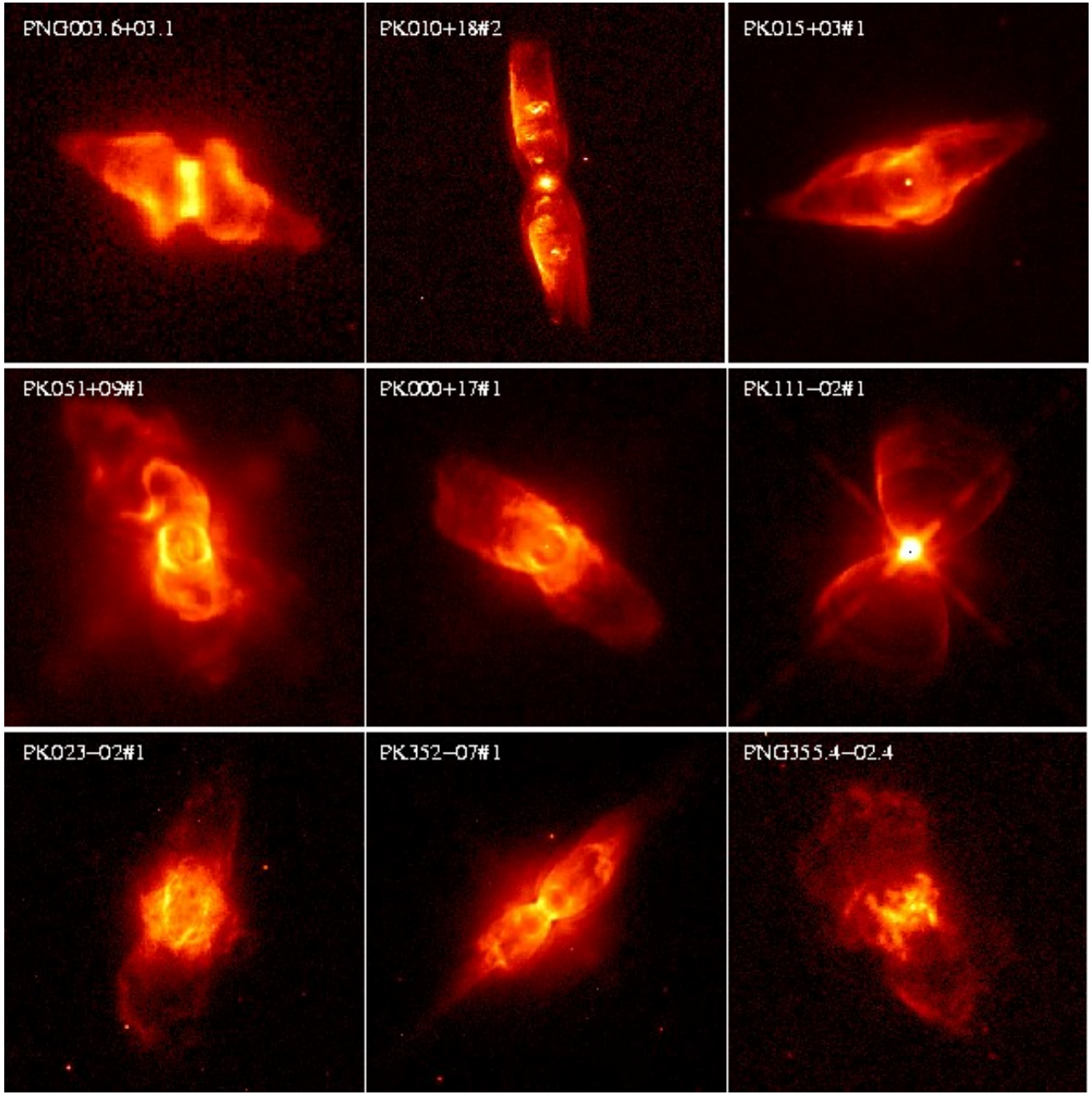

27% (32/117 objects)

Adapted from
Sahai, Morris & Villar (2011)

Primary Class L (collimated-lobe pair)

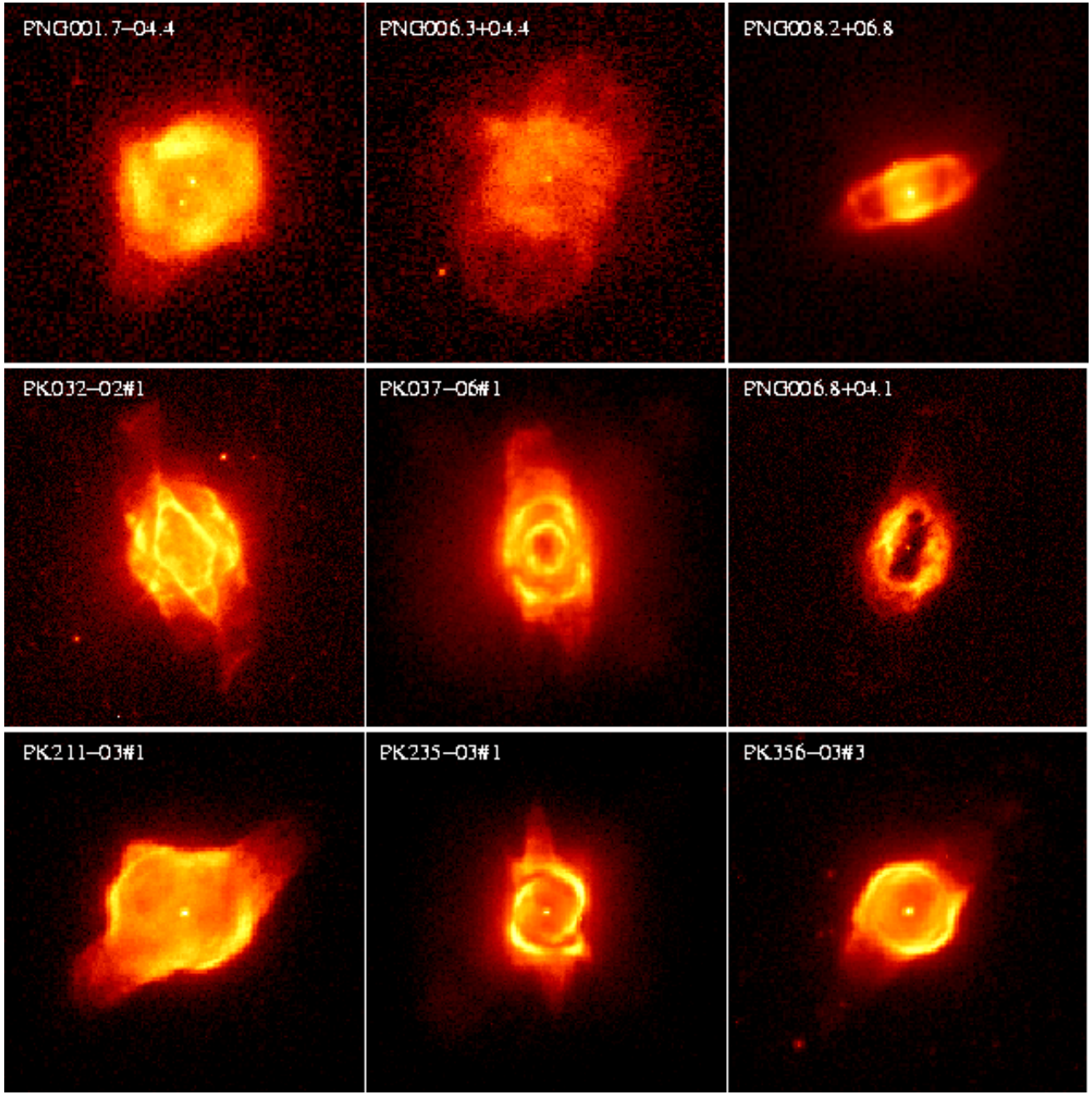

8.5% (10/117 objects)

Adapted from
Sahai, Morris & Villar (2011)

Note: closely related to class-B (but do not show pinched-in appearance where lobes join the waist region)

Primary Class M (multipolar)

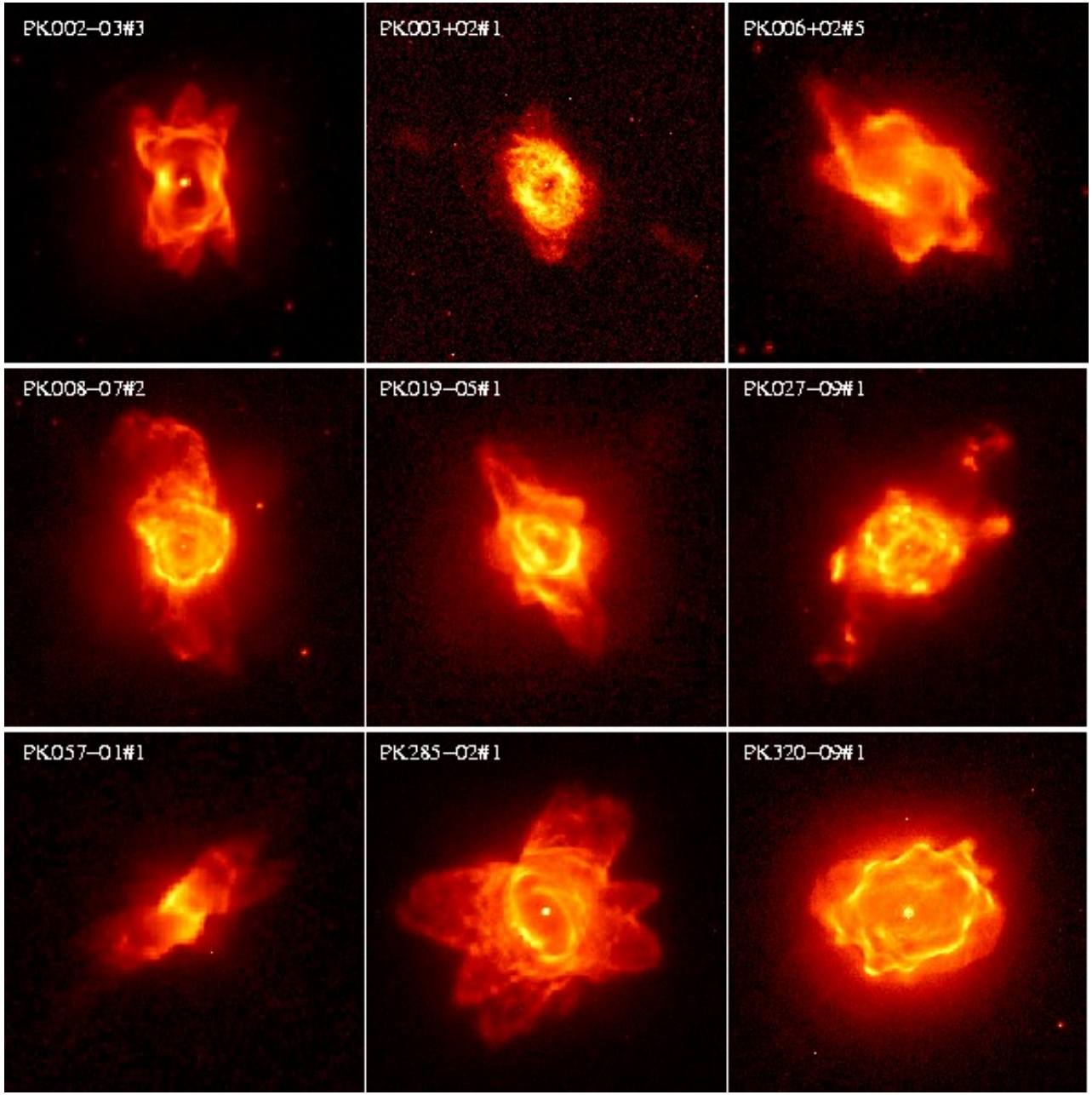

20% (23/117 objects)

Adapted from
Sahai, Morris & Villar (2011)

Primary Class E (elongated)

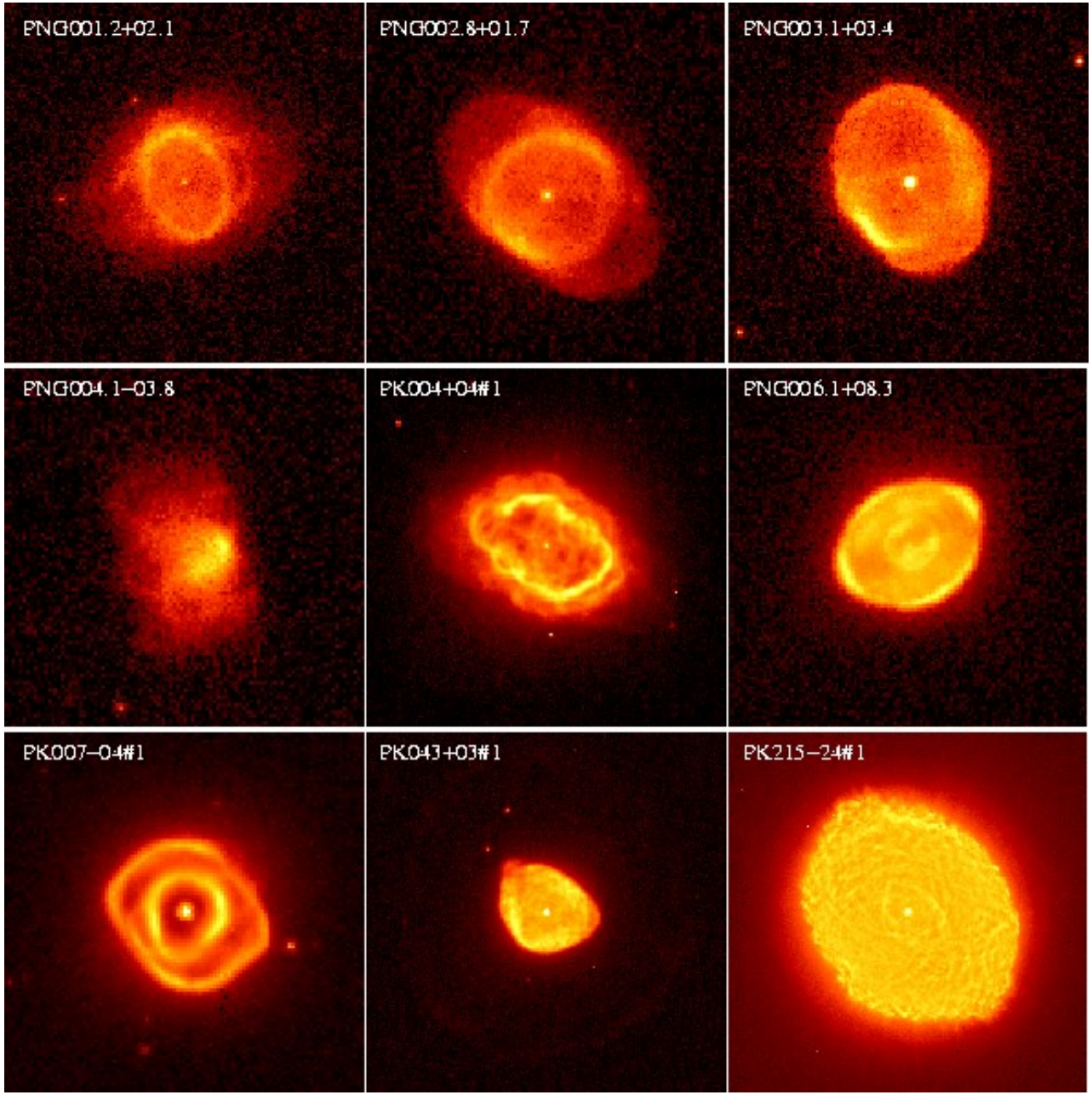

31% (36/117 objects)

Adapted from
Sahai, Morris & Villar (2011)

Note: class-B, L can look like class-E due to insufficient angular resolution and unfavorable orientation

Primary Class R (round)

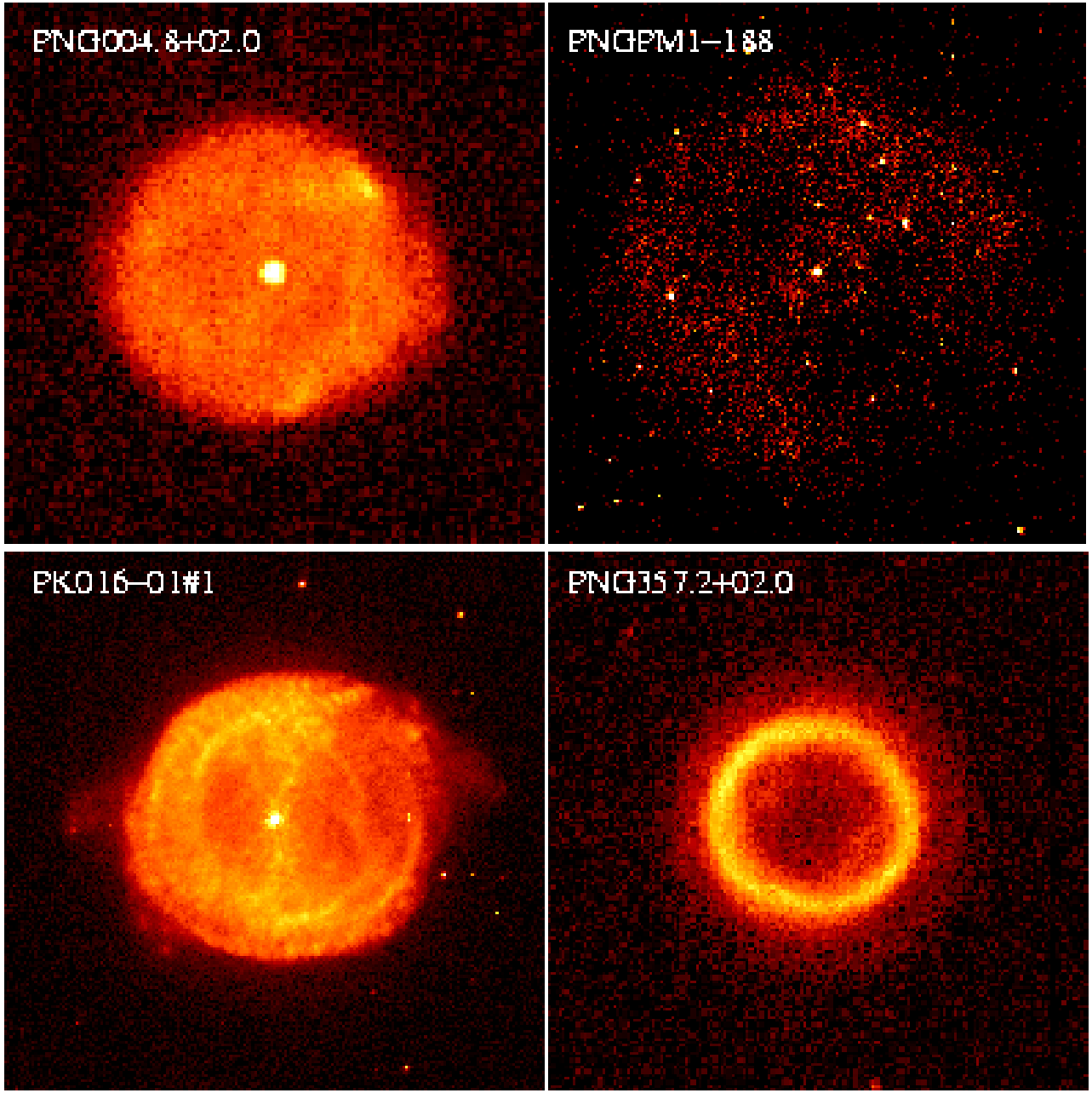

3.4% (4/117 objects)

Adapted from
Sahai, Morris & Villar (2011)

Primary Class S (spiral-arm)

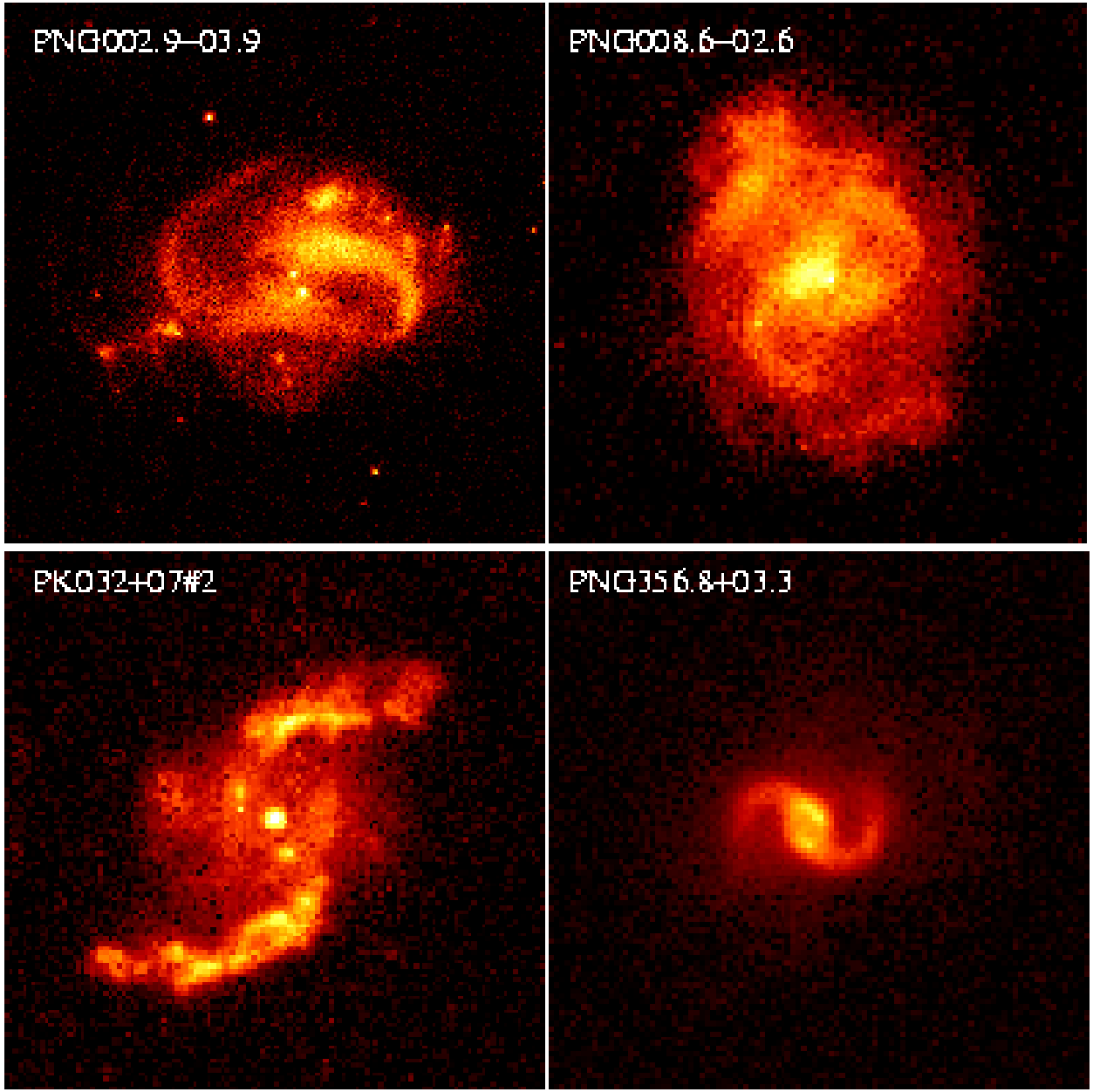

3.4% (4/117 objects)

adapted from
Sahai, Morris &Villar (2011)

Table 4:: Statistics

Classification	Number[1]	Fraction[1]	Number[2]	Fraction[2]
	$R_{exc} \leq 1$		All Objects	
B	27	0.28	33	0.28
M	18	0.19	23	0.20
E	32	0.34	37	0.31
I	6	0.063	8	0.068
R	4	0.042	4	0.034
L	7	0.074	10	0.085
S	2	0.021	4	0.034
	Point Symmetry			
B, ps[3]	12	0.44	14	0.45
M, ps[4]	15	0.83	19	0.83
E, ps[5]	13	0.41	15	0.42
ps[4]	42	0.44	53	0.45

1 2 3 4 5 6

[1]Number of objects in given class, and as a fraction of the total (96) for which the [OIII]λ5007/Hα flux ratio, $R_{exc} \leq 1$,

[2]Number of all objects in given class, and as a fraction of the total sample (119)

[3]Number of point-symmetric objects in class B, and as a fraction of the total in class B

[4]Number of point-symmetric objects in class M, and as a fraction of the total in class M

[5]Number of point-symmetric objects in class E, and as a fraction of the total in class E

B+M+L (extreme asphericity) fraction > ~55%!

Secondary characteristics important:

(a) Point-symmetry => secular trend such as precession or wobble in the orientation of the central engine or a collimated outflow

Note: different kinds of point-symmetry possible

(b) **Ansae** => impact of jet on slow-moving prior wind

(c) **Waist** => equatorial outflow or bound disk

(d) **Inner Bubbles** => reverse shocks, very hot gas

(e) **Barrel-shaped central Regions** => evolution of waist under impact from very fast wind from CSPN?

PN shapes/shaping: Primary Physical Processes (1)

Collimated (episodic) fast winds/ jets (CFWs), operating during the very late-AGB phase, interacting with round AGB circumstellar envelopes, are the primary agent which initiate the formation of aspherical shapes and structures (*Sahai & Trauger 1998*)

- highly collimated lobes, multipolar morphologies imply that fast outflows are probably born collimated (i.e. collimated at or very near the launch site)
- point-symmetry implies a secular trend in the orientation of the central driver of the CFWs (precession and/or wobble)
- very large momentum-excesses indicate that CFWs are not radiatively driven (*e.g. Bujarrabal et al. 2002*)

PN shapes/shaping: Primary Physical Processes (2)

- Dense waists seen in PPNe & PNe likely form during the late AGB phase. Huggins (2007) infers that waists and lobes formed nearly simultaneously, with waists forming a bit earlier **(***expansion timescales~few 100 to 1000 yr***)**
- (a) ionization by hot central star, (b) action of Spherical, Radiatively-Driven, Fast Wind (SRFW) *(speed ~1000 km/s)* from central star on the pre-shaped PPN is responsible for further morphological changes of the PN structure

lobe structures preserve shapes/geometries (since main morphological classes same in PPNe and young PNe)

major change due to expansion/ionization of dusty waist (SFRW, hot central star): waists become brightest components, central stars become visible

Fundamental Questions

- What are the origins and properties of the CFWs (~few x100 km/s) (e.g., scalar momentum, episodicity)?

- What is the origin and properties of equatorially-dense structures, i.e., the waists (bound/ expanding)? Physical mechanism is unknown - possibly common envelope ejection, or Bondi-Hoyle accretion of matter from AGB wind into a disk (determination of waist masses could provide a constraint)

- Is **Binarity** the underlying cause? [can lead to CE ejection, accretion disk formation, rotation, magnetic fields]

PNe & their Central Stars (X-Ray Emission)

CHANPLANS: First systematic survey of nearby (<~1.5 kpc) PNe with radii <~ 0.4 pc

CXO Cyc 12 (570ks) +14 (670ks) (e.g., Kastner+2012)

XMM Chandra

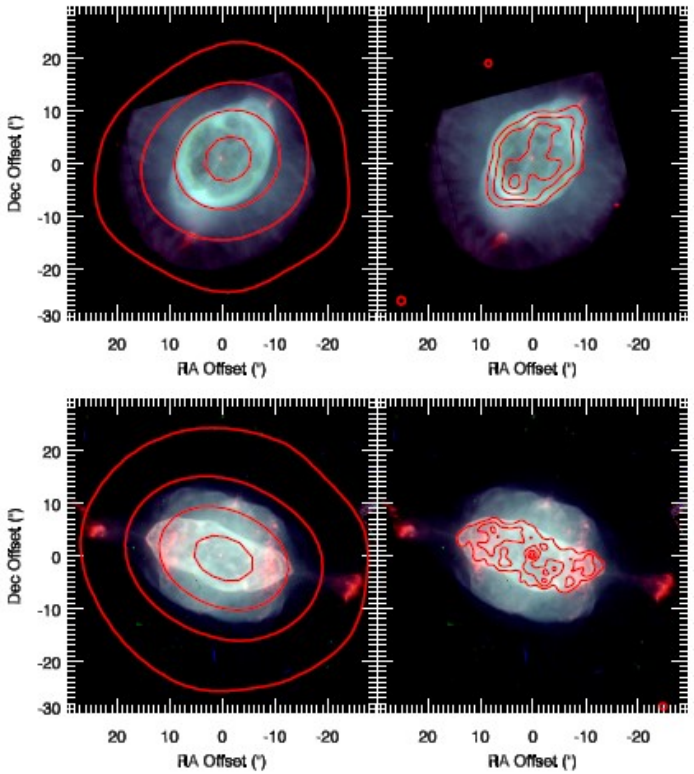

Hot-bubble X-ray emission from NGC3242 (top) and 7009 (bottom) overlaid on HST images (Kastner+2012)

IC418

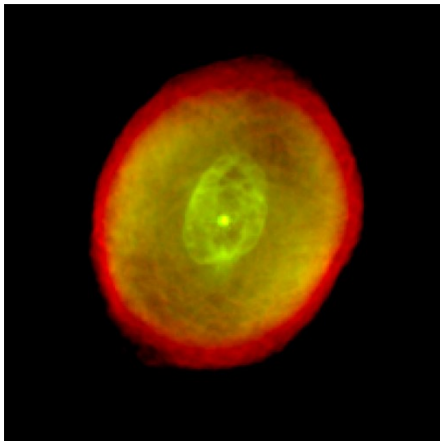

Inner-bubble in [OIII]5007 (green), Hα (red) HST image (SMV11)

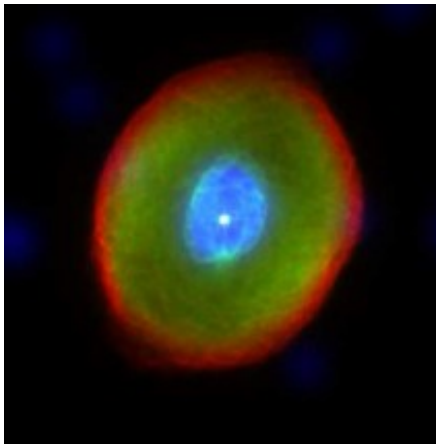

Hot-bubble in Xrays: CXO image (blue), Hα (green), [NII] (red) (Ruiz+2013)

- **(Expected)** Shocked gas due to a fast (~1000 km/s) wind from hot central star, interacting with slow wind ejecta, should produce a hot bubble at temperatures Tx >> 10^6 K
- **(New)** X-ray luminous central stars in 50% of PNe (70% for known binary CSPNe) - emission much harder (>~0.5 keV) than expected from stellar photosphere (100-200 kK)

Probe of processes related to central star (binarity and/or magnetic fields, or self-shocking winds as in O stars)

fuvAGB Stars (UV and X-Ray Emission)

Binaries with actively accreting main-sequence companions?

- **Search for binarity using FUV emission in AGB stars: Large and variable UV flux most likely related to accretion activity in a binary** (Sahai +2008)
- Pilot studies with XMM/Chandra to search for X-Ray Emission from fuvAGB Stars: 50% detection rate (Sahai+2014, in prep), energetic X-ray SEDs (coronal gas, Tx >30 MK, likely produced in an accretion shock, confined by magnetic fields in vicinity of AGB star/disk)

Y Gem: highest FUV flux amongst ~100 AGB stars with GALEX FUV fluxes (Sahai,Neill +2011)

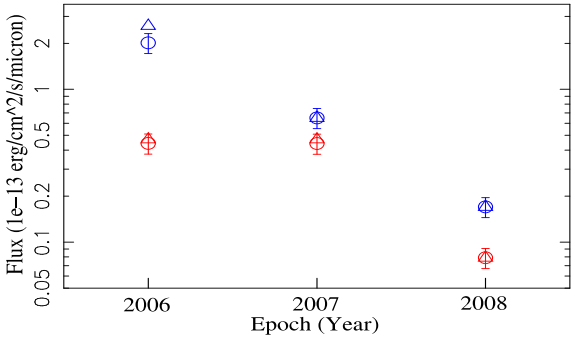

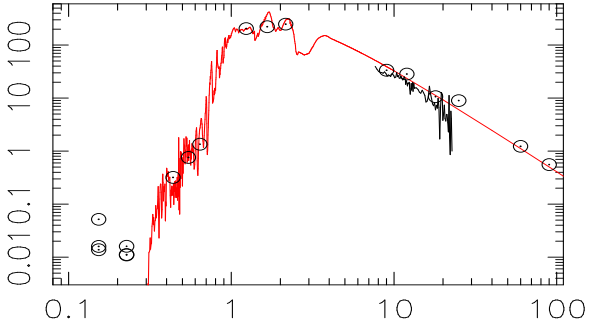

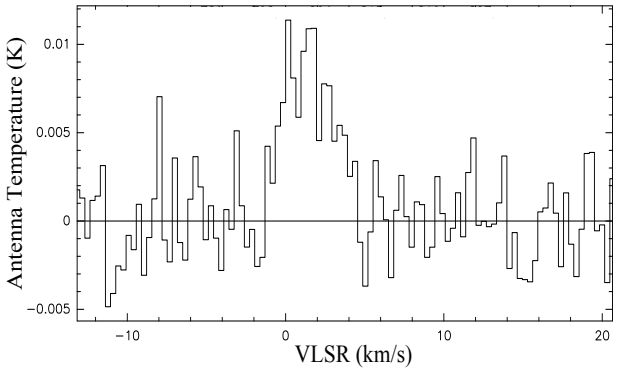

- Largest UV flux amongst all FUV-excess AGB stars (M8)
- UV flux very large, decreased dramatically from 2006 to 2008
- FUV/NUV flux ratio > 1
- **CO 2-1 line emission shows narrow profile** (FWHM=3.4 km/s) – likely arises in a large (~300 AU) disk, rather than a outflow (e.g., Jura & Kahane 1999)
- Hα profile variable on time-scales of days to months; radio emission shows thermal (ionized gas) & non-thermal emission
- Very energetic, variable X-ray SED (Tx~50-150 MK) , **Fe 6.3-6.9 keV line emission - X-rays scattered by disk?**

pAGB Objects (Dusty Equatorial Waists)

Dusty Waists - important morphological component of post-AGB objects

2 major classes of post-AGB objects

(a) PPNe different in their morphologies (have extended outflows)

(b) disk-prominent post-AGB objects (dpAGB): (radial-velocity) binary stars and circumbinary disks (lack extended nebulae). (e.g., AC Her, U Mon, RV Tau unresolved, <1"-2": *Sahai, Claussen, Schnee, & Morris 2011*)

- 2 Different OBSERVED Manifestations of such structures

1. Large (~1000 AU) Torii

i) Dark band obscuring central star in a bipolar/ multipolar object (mostly PPNe); in some cases, an outer radial edge is detected

ii) Bright toroidal or barrel-shaped regions (in most PNe)

2. Medium-sized (~10-50 AU) Disks

Disks in dpAGB objects (*e.g., proposed from SED/spectral modelling: e.g., de Ruyter+2005; van Winckel +2008, Gielen+2007; direct detection - interferometric visibilities with VLTI & modelling , e.g., Lykou+2011,* Keplerian disk with CO interferometric observations (Red Rectangle) e.g., *Bujarrabal+2013*)

pAGB mass loss (Dusty Equatorial Waists)

- The origin of these circumbinary disks and large dusty waists is a mystery

current models based on Bondi-Hoyle accretion from an AGB wind around a companion only produce small-sized (~1 AU) accretion disks (*Mastrodemos & Morris 1998,1999*)

But, the waist regions of PPNe and dpAGBs share many observational similarities

a) Submm excesses: large (millimeter-size) grains

b) Crystalline silicate features (e.g., seen in Spitzer spectra: *Gielen+2007*)

So, in both PPNs and dpAGBs, the mineralogy and grain sizes show that dust is highly processed

- Probe the mass/kinematics of the dust/waist structure => test formation models

low mass & Keplerian rotation (e.g. due to accretion around a companion from AGB wind)

large mass & expansion, if Common Envelope ejection in a binary, equatorial mass-outflow

waist lifetime > time-scales for dust processing, grain growth (> ~ 2000 yr, *Jura 2001*)

pAGB mass-loss: Continuum Emission from Dusty Waists

Pilot Study (*Sahai+2011*)

Table 1: Radio and Millimeter-Wave Fluxes of post-AGB Objects

Source	X μJy(σ)	Ka μJy(σ)	Q μJy(σ)	3 mm[a] mJy(σ)	1.3 mm[b] mJy(σ)	0.85 mm mJy(σ)	D[c] kpc	M_d $10^{-2} M_\odot$
RV Tau	...	270 (50)	(107)	3.9(0.2)	...	50.3 (3.6)[d]	2.2	0.1
U Mon	...	(100)	(169)	15(0.3)	100(14)	182 (2.6)[d]	0.77	0.064
AC Her	(46)	...	...	4.6(0.4)	38(1)	99.4 (3.8)[d]	1.1	0.072
IRAS16342−3814	(162)	(168)	(254)	...	277 (13)[e]	602 (90)[f]		
IRAS17150−3224	...	(240)	(213)	...	158 (10)[e]	...		
IRAS18135−1456	(66)	(82)	(169)	12 (1.4)[g]	...	...		
IRAS18276−1431	...	(108)	(157)	11 (3.2)[g]	...	...		
IRAS19548+3035	(45)	...	...	6 (1.1)[g]	...	...		
IRAS20000+3239	(44)	...	...	6 (1.1)[g]	11.4(1.7)[h]	30.9 (2.5)[i]		
IRAS22036+5306	1010 (62)	1180 (55)	1230 (81)	8.4 (0.7)[j]	...	290 (40)[j]	2	2.2

[a] Beam sizes for RV Tau, U Mon, & AC Her 3 mm observations are 2.″4×1.″5, 2.″4×2.″1, & 2.″4×1.″5, respectively

[b] Beam sizes U Mon & AC Her 1.3 mm observations are 2.″2×0.″9 & 2.″0×1.″8, respectively

Confirm presence of substantial masses of very large (mm-size) grains

β at mm wavelenghts lower in dpAGBs (<0.4) than PPNe (~1)

Extended study in progress using SMA, CARMA, ALMA, ATCA, VLA (huge increase in sensitivity): *Sahai, Patel, Gonidakis et al 2014, in prep*

AGB Mass-Loss: *extended CSE structure signature of hidden binary at center*

"Circular Arcs" or Archmidean Spiral Structure

First seen in many well-known AGB/pAGB objects with HST (IRC 10216, CRL 2688, NGC 6543, NGC7027)

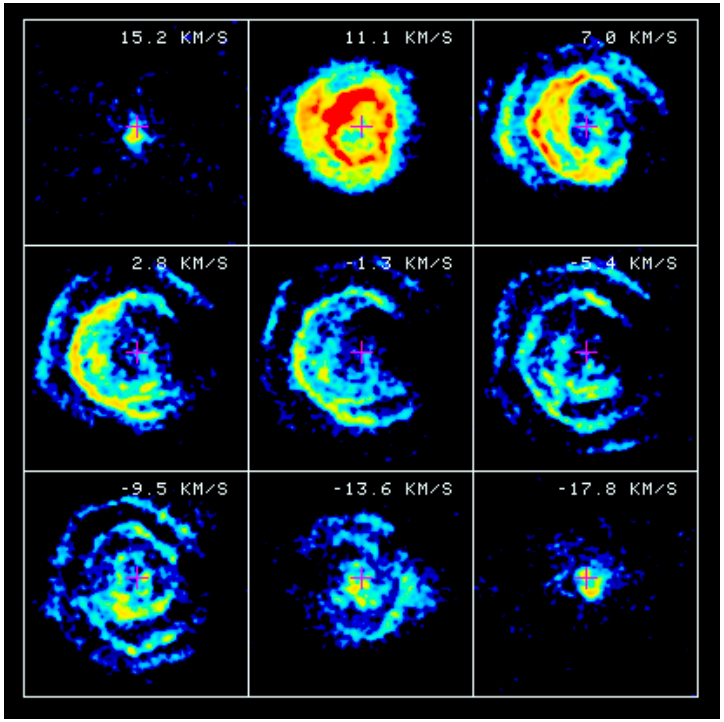

CIT-6 HC3N J=4-3 (36.39 GHz)
beam ~0.7" x 0.6", panel size 21"
Claussen, Sjouwerman, Rupen et al. 2011)
a one-armed spiral in the center?
(inferred by *Dinh-V-Trung & Lim 2009*, from a lower-resolution map)

Spiral structure can be induced by a companion
(first shown by *Mastrodemos & Morris 1999*)

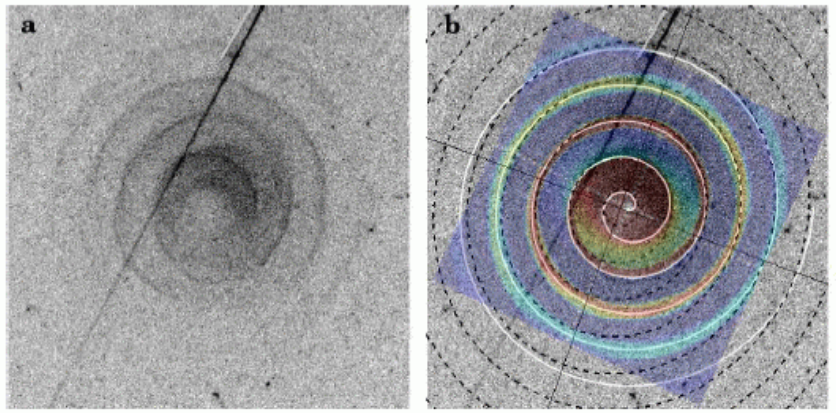

CRL3068 HST image: *Morris+2006, Mauron & Huggins 2006*

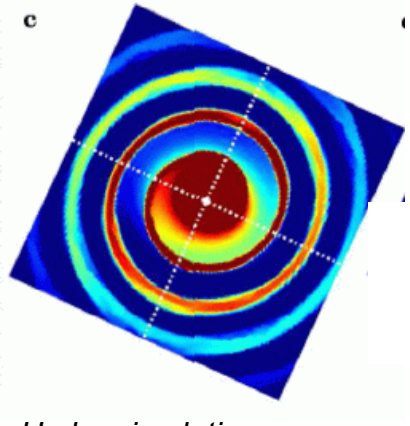

Hydro simulation: comparable mass binary system, orbital plane inclined by 50 deg (Kim & Taam 2012)

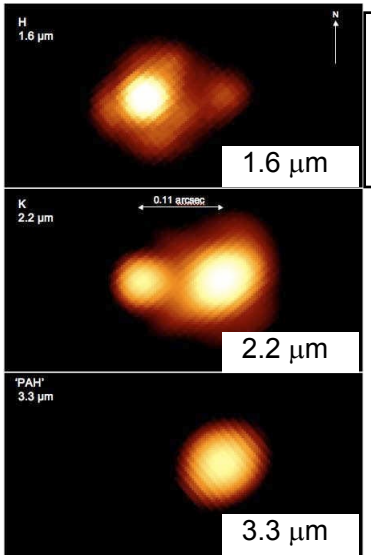

Central binary in CRL3068 (Keck AO: *Morris+2006*)

(see also ALMA observations of R Scl, Maercker+2012)

AGB mass-loss (duration, total mass of ejecta)

(mass~R_{out}, outer boundary probed via signature of ISM interaction)

GALEX FUV/NUV image of IRC10216 (*Sahai +Chronopoulos 2010*)

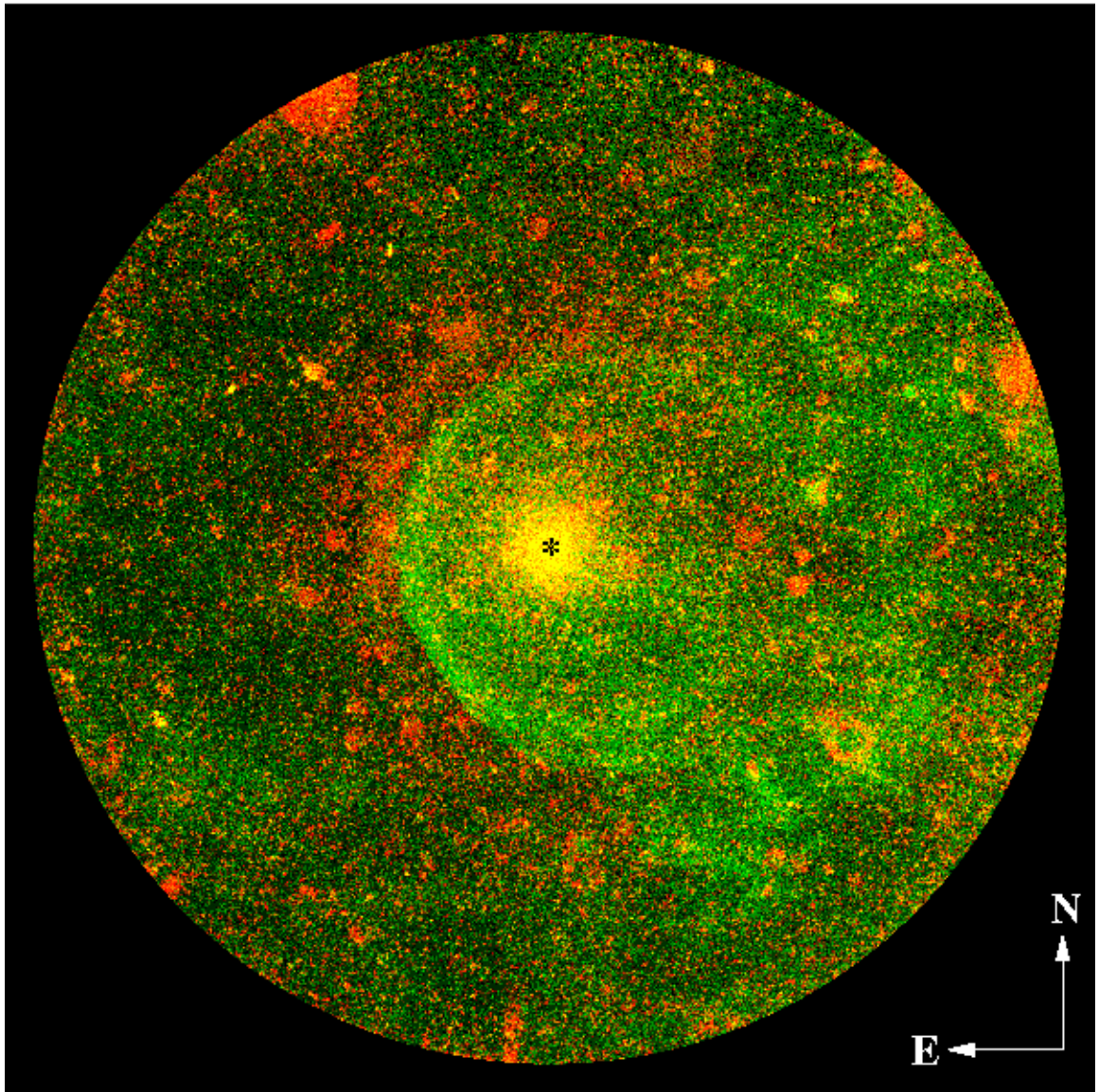

- AGB CSEs much larger than traced in CO (photodissociated by Interstellar UV)
- Scattered light from dust traced further out with deep optical imaging (200” for IRC10216)
- even further out, HI observations useful (but difficult!)

Bow-shock shows evidence of interaction with ISM at radii 500”-1000” (termination shock to bow-shock)

Envelope Mass (*taking dM/dt=2 x 10^{-5} Msun/yr, d=130 pc*) is > ~1.4 Msun

Such observations provide, for the first time, a physical outer boundary to the CSE resulting from dense, heavy AGB mass-loss

e.g., Bow-shocks in R Cas, R Hya, α Ori, Ueta+2010 (& references therein)

AGB mass-loss (duration, total mass of ejecta)

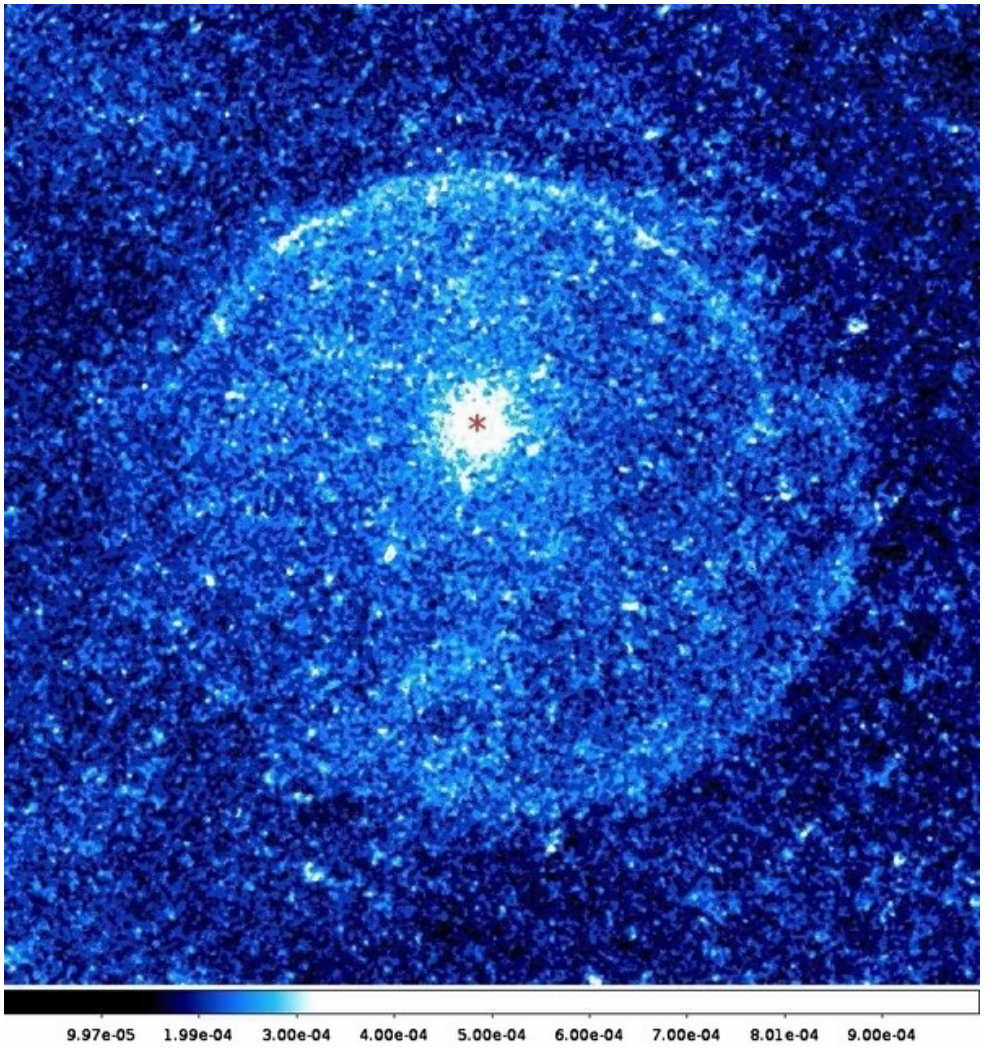

FUV *GALEX* image of CIT 6 (24'.75 × 24'.75)

(location of the central star: *)

Astrosphere of carbon star CIT 6

(*Sahai & Mack-Crane 2014*)

Total Envelope Mass > ~0.3 Msun

Object moving North thru Warm Ionized Medium at >~ 39 km/s

Puzzling Features

Double-arc structure, detailed shape of astrosphere not well explained by models

- Higher mass-loss rate in past?
- Inclination?
- Object has entered relativelu dense clump of WIM recently

AGB Mass Loss (duration, total mass of ejecta)

Herschel PACS imaging

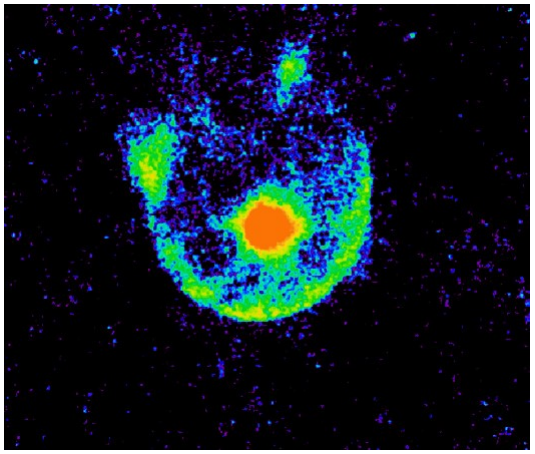

Fermata: UU Aur

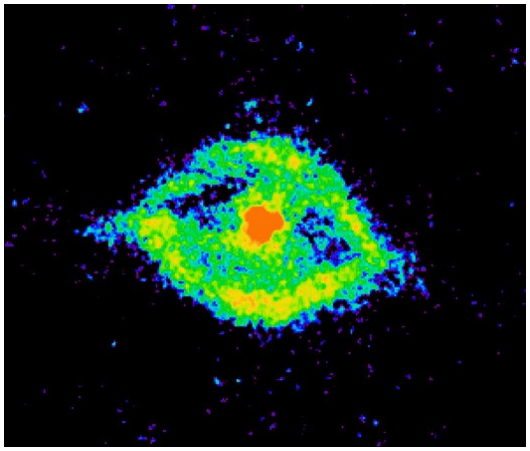

Eyes: VY Uma

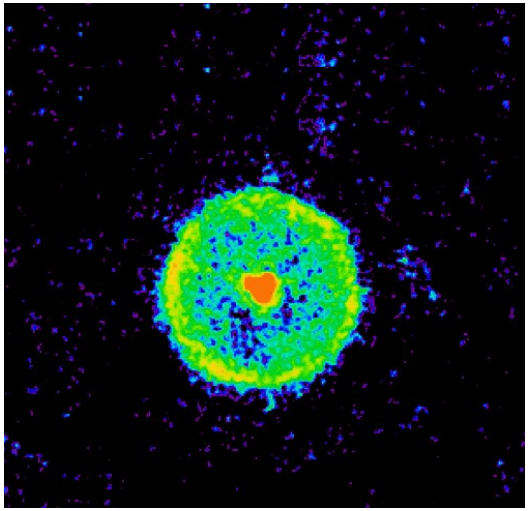

Rings: AQ And

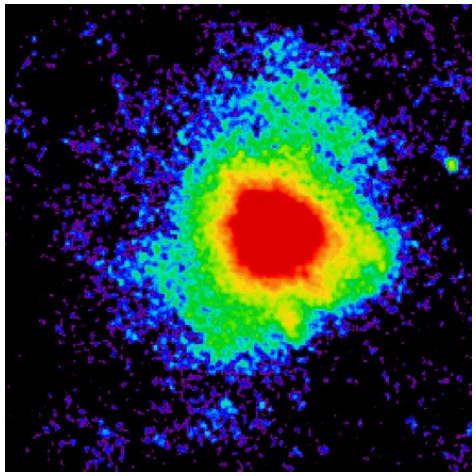

Irregular: V Cyg

Cox+2012: PACS 70 and 100 μm imaging (part of the MESS Key program: PI Groenewegen)

For 43/56 nearby (<0.5 kpc) AGB and supergiants:

- *Fermata* and *eyes* due to bow-shock interactions of the AGB winds with the ISM
- *Eye*-class tentatively associated with (visual) binaries
- *Rings* do not appear in M-type stars, only for C or S-type stars, consistent with their origin being a thermal pulse
- 3 stars (R Scl, TX Psc, U Cam) show *rings* and evidence of bow-shock interaction

Detailed modeling using hydrodynamical simulations to fit stand-off distance, shape, density distribution, e.g., Villaver+2012

Bow-shock: Standoff distance

~ $(dM/dt \; V_{exp} / n_{ISM})^{0.5} / V_*$ (V_* is velocity relative to ISM)

pAGB mass-loss: Herschel/HIFI observations

PPNe and PNe (**HIFI Key Herschel Program,** *Bujarrabal+2012*)

CRL618

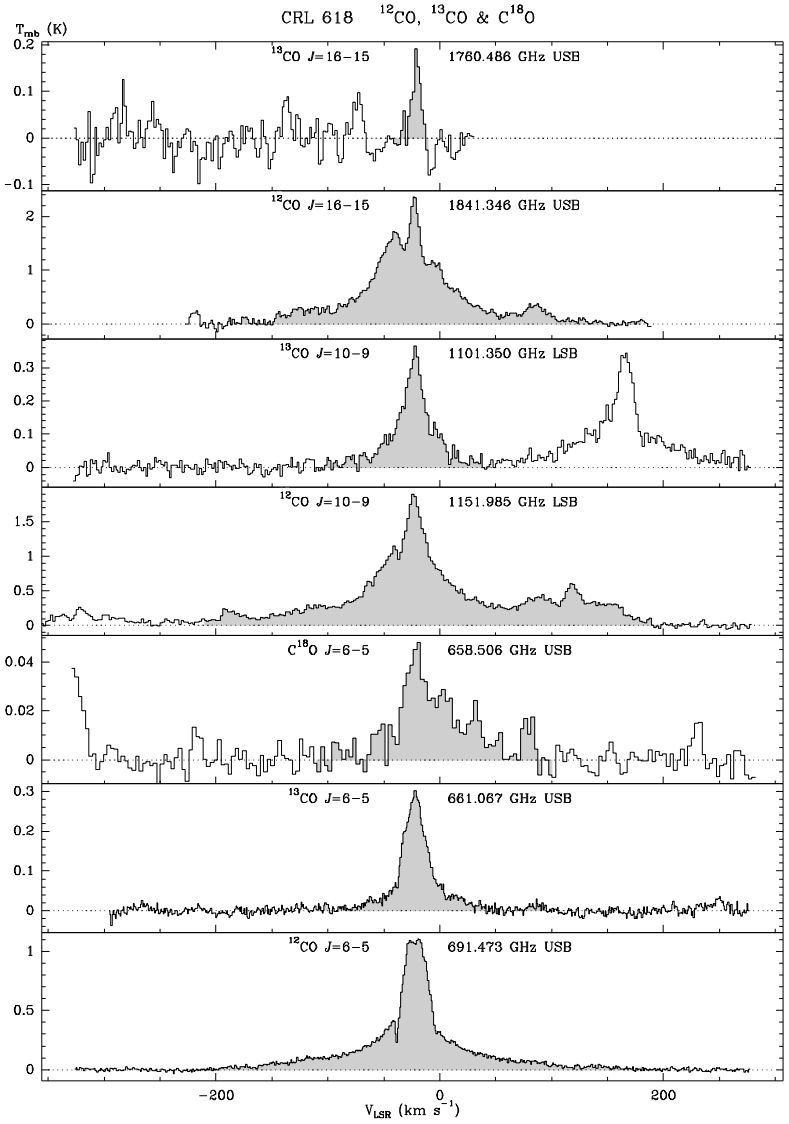

Wide profiles, sometimes very extended wings

OH231.8+4.2

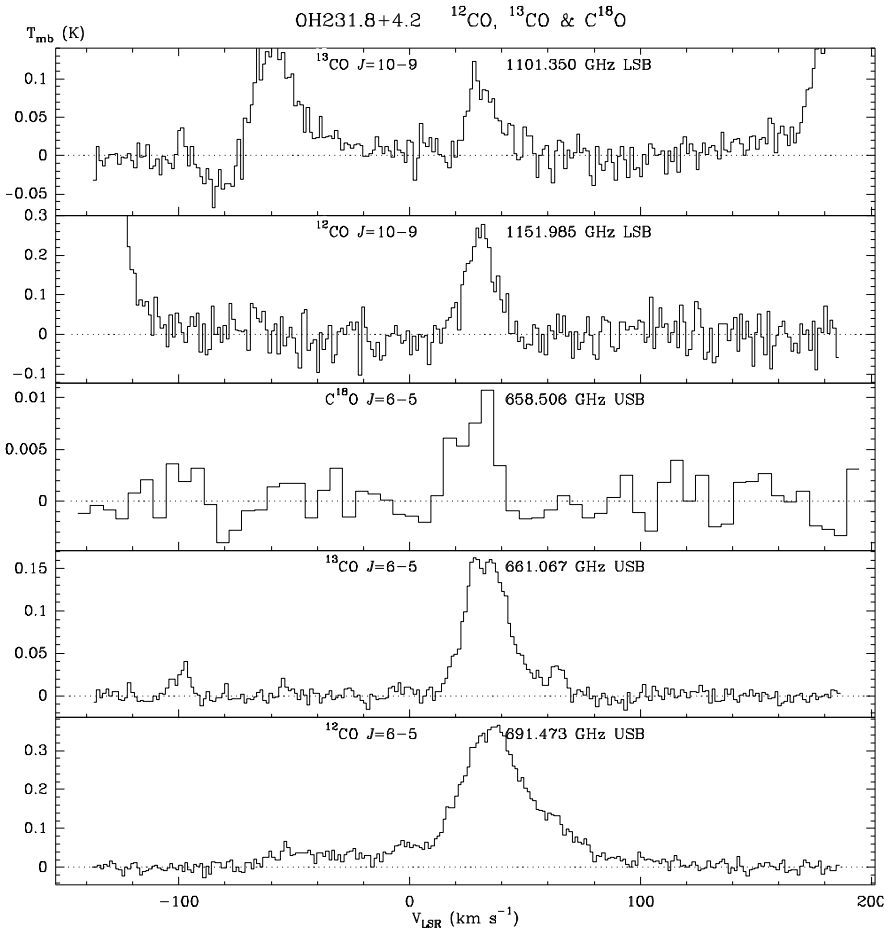

Submm & Far-IR lines from CO, ^{13}CO, H_2O (and others)

Warm fast winds (CRL618: >200K, CRL2688: 100K)

Cold fast winds (OH231.8+4.2, NGC6302: 30K)

=> cooling of the fast wind with age: fast outflow *in* CRL618 is young (100 yr), in OH231.8, older (1000 yr)

pAGB mass-loss: OPACOS Survey

S'anchez Contreras & Sahai 2012

20 pPNe (+5 AGBs, 2 PNe)

Properties of the Sources in Our Survey OPACOS

Source (IRAS No.)	Other Names	Object[a] Class	Spectral Type	Morphology[b] (Opt./NIR)	Chemistry[c]	f_{12}/f_{25}	f_{60} (Jy)	d[d] (kpc)
03206+6521	OH 138.0+7.2	AGB	M?	S	O	0.71	37.5	3.4
18055−1833	V* AX Sgr	PPN	G8Ia	S	O	0.73	33.1	2.0
18135−1456	OH 15.7+0.8	PPN	G5-K0	S	O	0.25	158	2.5
18167−1209	OH 18.5+1.4	PPN	F7	S	O	<0.16	21.3	7.0
18276−1431	OH 17.7−2.0	PPN	A0-K5	B	O	0.17	120	3.0
18348−0526	OH 26.5+0.6	AGB	M	†	O	0.57	463	1.1
18420−0512	OH 27.5−0.9	PPN	M1	B,ml	O	0.04	26.2	6.0
18460−0151	OH 31.0−0.2	PPN(wf)	...	†	O	<0.64	<277	7.0
18560+0638	OH 39.7+1.5	AGB	M	†	O	0.83	101	1.4
19024+0044	OH 35.3−2.6	PPN	G0-5	M	O	0.06	42.5	10
19134+2131		PPN(wf)	...	B	O	0.32	8.56	8
19234+1627	PN G051.5+00.2	PN	...	E	...	<0.22	15.5	9.5
19255+2123	OH 56.1+2.1,K3-35	PN	>60kK	B	O	0.08	48.2	4.0
19292+1806	OH 53.6−0.2	PPN	B?	B	O	<0.10	28.8	5.0
19306+1407		yPN	B0-1	B	C+O	0.06	31.8	5.5
19374+2359		yPN	B3-6	B	O	0.24	70.9	11
19475+3119	HD331319	PPN	F3	M	O	0.01	55.8	3.5
19548+3035	RAFGL2477	PPN	M6	S	C+O	0.69	46.7	4.0
19566+3423		AGB	...	S	C+O	0.42	49.0	9.0
20000+3239	GLMP 963	PPN	G8I(simb)	E/B	C	0.21	30.0	3.0
20462+3416	LS II+34 26	yPN	B1.5	E	O	:0.02	12.1	2-5
22036+5306	GLMP 1052	PPN	F4-7	B	O	0.18	107	4.0
22177+5936	OH 104.9+2.4	AGB	M	S	O	0.54	90.7	2.4
22223+4327	V448 Lac	PPN	F8Ia	B	C	0.06	22.4	4.0
22568+6141	PN G110.1+01.9	yPN	B0	B	...	0.12	20.8	6.0
23166+1655	AFGL3068, LL Peg	AGB	C	spiral	C	0.91	248	1.1
23304+6147	GLMP 1078	PPN	G2Ia	B(M?)	C	0.19	26.6	4.0

Many interferometric CO mapping papers by Bujarrabal, Alcolea , S'anchez Contreras, Castro-Carrizo & colleagues on post-AGB objects such as M1-92, M2-56, CRL618, IRAS19475, Red Rectangle …

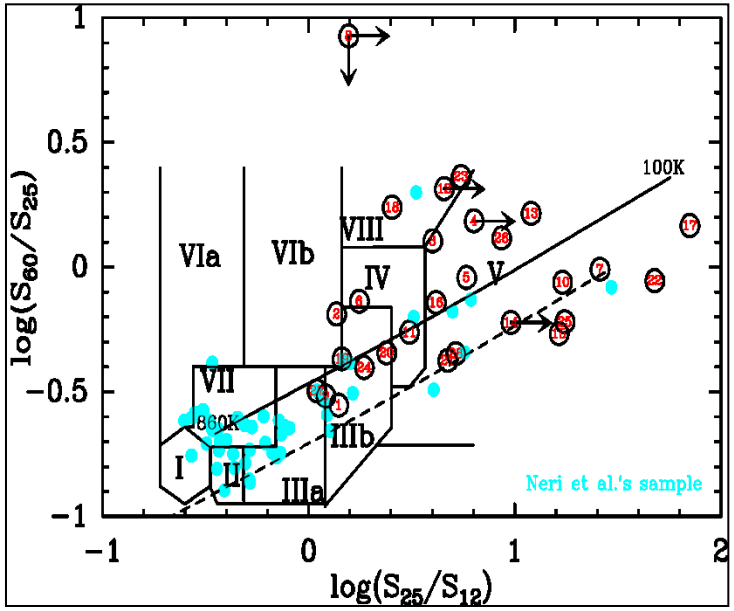

Objects have extended, cool dust shells

SUMMARY OF OBSERVATIONAL RESULTS

Circumstellar ^{12}CO: 24 detections (+ 3 upper limits) - sample of PPNe with CO data significantly enlarged - envelope spatially resolved in ~18/24 objects - asymmetries and velocity gradients in all; broad wings in line profiles for ≥ 50% (=> *signatures of fast post-AGB outflows*)

Surveys lead to discoveries of extreme objects, e.g., IRAS19374, which have very large momentum excesses, and thus provide the most stringent tests of theoretical models